

# Low-Light Image Enhancement via Self-Reinforced Retinex Projection Model

Long Ma, Risheng Liu, *Member, IEEE*, Yiyang Wang, Xin Fan, *Member, IEEE*, and Zhongxuan Luo

**Abstract**—Low-light image enhancement aims to improve the quality of images captured under low-lightening conditions, which is a fundamental problem in computer vision and multimedia areas. Although many efforts have been invested over the years, existing illumination-based models tend to generate unnatural-looking results (e.g., over-exposure). It is because that the widely-adopted illumination adjustment (e.g., Gamma Correction) breaks down the favorable smoothness property of the original illumination derived from the well-designed illumination estimation model. To settle this issue, a great-efficiency and high-quality Self-Reinforced Retinex Projection (SRRP) model is developed in this paper, which contains optimization modules of both illumination and reflectance layers. Specifically, we construct a new fidelity term with the self-reinforced function for the illumination optimization to eliminate the dependence of the illumination adjustment to obtain a desired illumination with the excellent smoothing property. By introducing a flexible feasible constraint, we obtain a reflectance optimization module with projection. Owing to its flexibility, we can extend our model to an enhanced version by integrating a data-driven denoising mechanism as the projection, which is able to effectively handle the generated noises/artifacts in the enhanced procedure. In the experimental part, on one side, we make ample comparative assessments on multiple benchmarks with considerable state-of-the-art methods. These evaluations fully verify the outstanding performance of our method, in terms of the qualitative and quantitative analyses and execution efficiency. On the other side, we also conduct extensive analytical experiments to indicate the effectiveness and advantages of our proposed model. Code is available at <https://github.com/LongMa319/SRRP>.

**Index Terms**—Low-light image enhancement, image denoising, illumination estimation.

## I. INTRODUCTION

Although, many computer vision fields, like visual tracking [1], action recognition [2] and others [3] are urgently thirst for high-quality images, the quality of images is rifely weakened by various factors including low-lightening conditions.

This work is partially supported by the National Natural Science Foundation of China (Nos. 61922019, 61733002, and 62027826) and the Fundamental Research Funds for the Central Universities.

L. Ma is with the School of Software Technology, Dalian University of Technology, Dalian, 116024, China. He is also with the Peng Cheng Laboratory, Shenzhen, 518052, China. (e-mail: malone94319@gmail.com).

R. Liu is with the DUT-RU International School of Information Science & Engineering, Dalian University of Technology, Dalian, 116024, China. (*Corresponding author*, e-mail: rsliu@dlut.edu.cn).

Y. Wang is with the College of Artificial Intelligence, Dalian Maritime University, Dalian, 116026, China. (e-mail: yywerica@dlmu.edu.cn).

X. Fan is with the DUT-RU International School of Information Science & Engineering, Dalian University of Technology, Dalian, 116024, China. (email: xin.fan@dlut.edu.cn).

Z. Luo is with the School of Software Technology, Dalian University of Technology, Dalian, 116024, China. (email: zxluo@dlut.edu.cn).

Manuscript received January 19, 2021; revised August 20, 2021.

Over the years, people have made a lot of efforts for improving the quality of low-light images. However, the process of gaining high-quality images from low-light observations usually contains uncertainties and unknowns.

The mainstream of existing low-light image enhancement techniques ([4], [5], [6], [7], [8], [9], [10], [11], [12], [13]) is developed based on the illumination inference. The key of these work lies in the design of regularizations of either data priors or physical priors. However, the illumination adjustment (e.g., Gamma correction) is always adopted to further improve the illumination obtained from the designed model or network. Although the additional operation of the illumination adjustment helps improve the final enhancement, it brings unclear details and inappropriate exposures since the mapping changes the original favorable smoothness of the derived illumination.

In this work, we develop a novel illumination-based model. Our algorithm is performed with great-efficiency and high-quality, meanwhile, it successfully avoids using the illumination adjustment skills (e.g., Gamma Correction (GC)). Here, we showed an example to illustrate the drawback of illumination adjustment. As shown in Figure 1, we used the commonly-used operator Relative Total Variation (RTV) [16] to generate the smoothed illumination. It can be seen that the adjusted illumination by GC indeed suppresses the over-exposure. Nevertheless, as indicated in the last row of Figure 1, the details in the zoomed-in region become blurred. Further, GC changes the distribution of original smoothed illumination in some regions as shown in the 1D signal curve (i.e., bottom row). We also considered the well-known illumination-based method LIME [8], whose result is worse because the over-and under-exposure all occurred in different regions.

More concretely, as shown in the subfigures (c)-(e) of Figure 1, in terms of the second row, the GC indemnifies the outstanding edge-aware smoothness, which is derived from an image smoothing model. As for the second row of the subfigure (c), the red line (the initial illumination, i.e., the v-channel of low-light input) and green line (the original smoothed illumination) almost kept the same difference between in [250, 500] and [0, 200]. However, in terms of the revised illumination by GC (i.e., the blue line), the promotion of pixel values in [250, 500] was significantly higher than [0, 200]. It shrank the inherent difference between different goals (e.g., the flower and the tower) to break down the excellent smoothing property. Further, as it can be observed in the second row of the subfigure (d), the blue line was over-smoothing, leading to the existence of over-exposure and under-exposure (pay attention to the tower and the white cloud). Compared with them, our SRRP (i.e., the subfigure (e)) successfully overcame

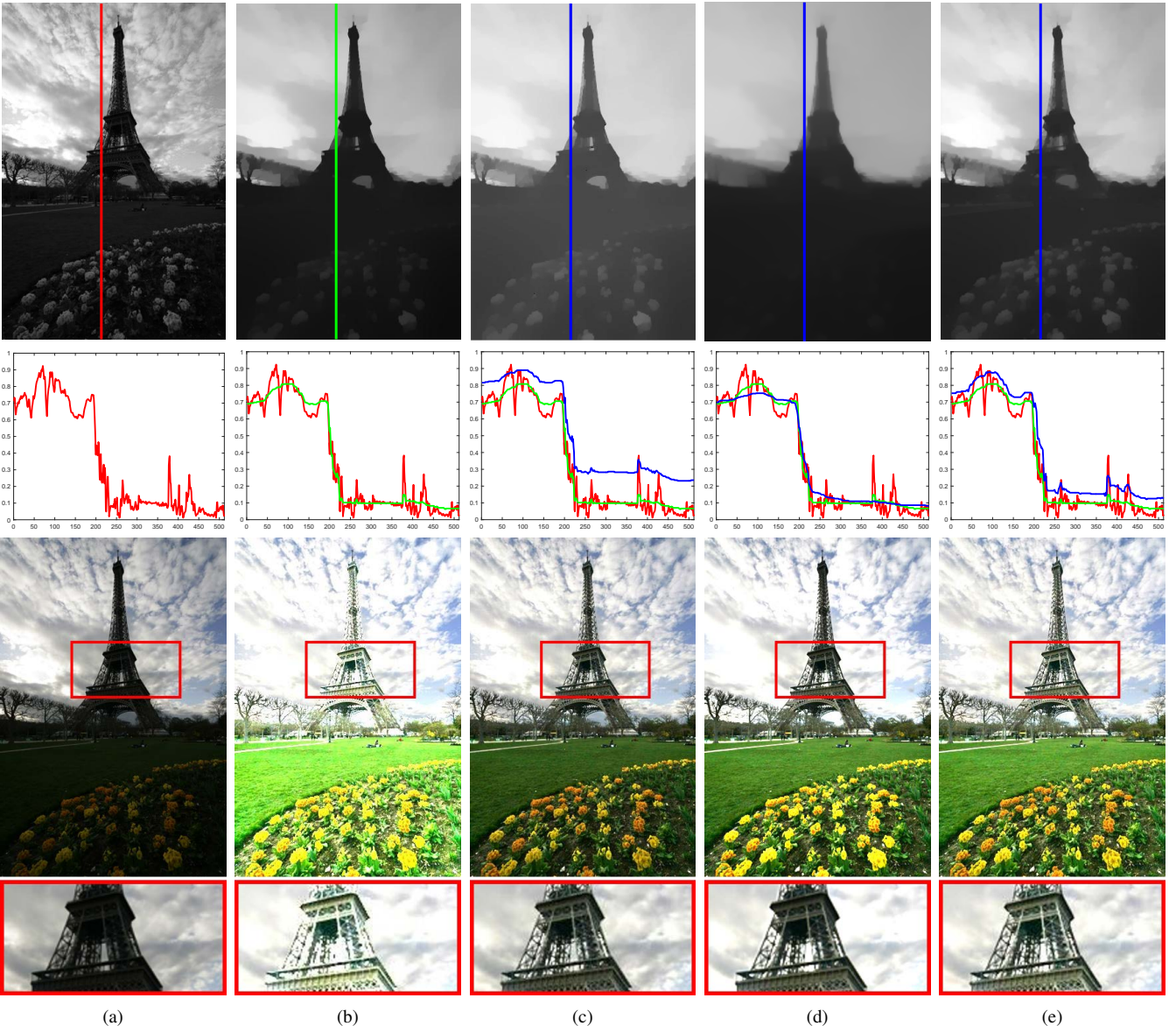


Fig. 1. Analyzing the illumination adjustment. (a) represents the low-light input; (b) represents the results by using Relative Total Variation (RTV); (c) represents the results by performing Gamma Correction ( $\gamma$  is empirically set as 2.2) on (b); (d) represents the results of LIME [8]; (e) is our SRRP. **Top**, **Middle**, and **Bottom** are the estimated illumination, the 1D curve of the color line in the corresponding illumination, reflectance, respectively. The second row of (a) represents the 1D curve of the red line marked in the first row of (a), and it is also presented in the 1D curves of (b)-(e). In the second row of (b), the green curve represents the 1D curve of the green line marked in the first row, and it is presented in the 1D curves of (c)-(e). In the second row of (c)-(e), the blue curve represents the 1D curve of the blue line marked in the first row.

these issues and achieved the better performance. This figure fully verifies the effectiveness of our proposed algorithm.

Furthermore, Figure 2 shows two groups of results in two low-light images captured in different natural imaging environments. The top and bottom rows are the front-lighting and back-lighting real-world scenarios, respectively. As far as the top row, the result of LIME [8] (a classical illumination-based traditional model) performs over-exposure. RetinexNet [14] (an illumination-based network) generates unnatural results. EnlightenGAN [15] (an illumination-free GAN-based method) produces some inevitable blurs and sensible artifacts. Compared with them, our result has the best visual effects with appropriate exposure, especially in the zoomed-in regions. In regard to the bottom, as the zoomed-in regions demonstrate,

all these compared methods fail to generate sufficient details, while our result still obtains a satisfactory performance.

In this paper, we develop a Self-Reinforced Retinex Projection (SRRP) model which contains the illumination and reflectance optimization modules. A self-reinforced function is introduced to get rid of the dependence of the illumination adjustment. A flexible feasible constraint is introduced in the reflectance estimation to obtain a reflectance optimization module with projection. We provide an enhanced version of our proposed SRRP to effectively handle the noises/artifacts generated in the procedure of enhancement. Extensive evaluations of different real-world scenarios show our superiority against other state-of-the-art approaches. Our main contributions can be concluded as

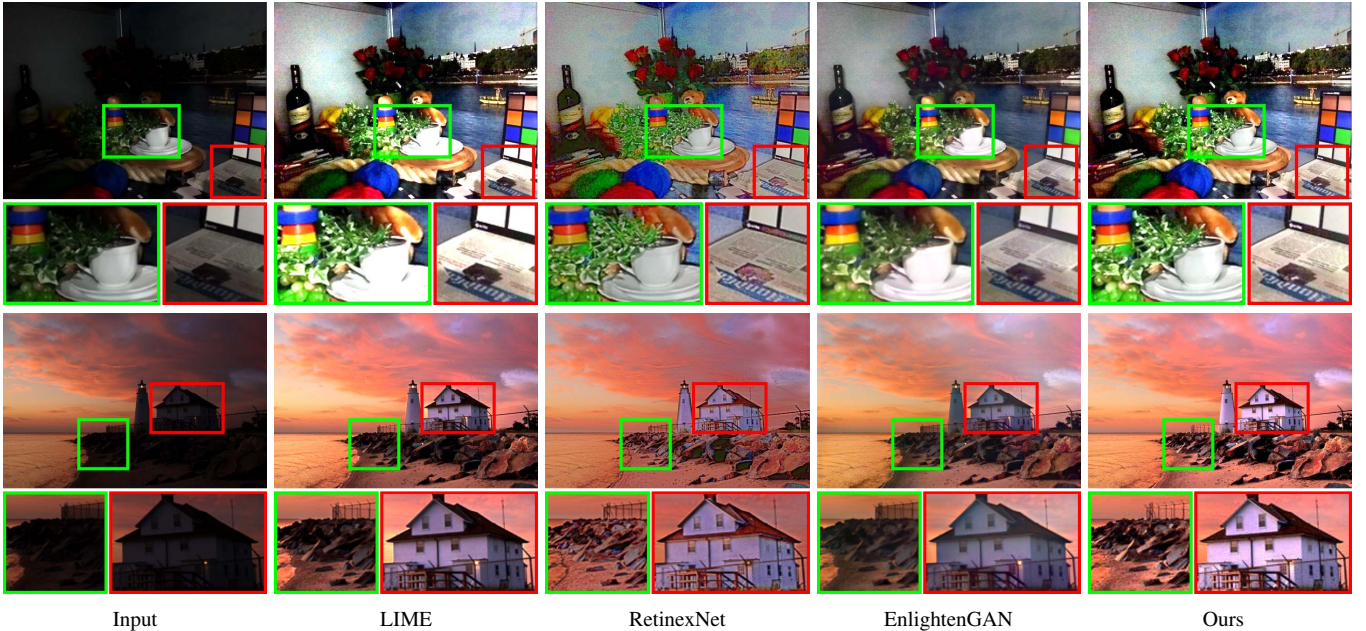


Fig. 2. Visual comparison of our method with LIME [8], an illumination-based traditional method, RetinexNet [14], an illumination-based network (paired supervision), and EnlightenGAN [15], an illumination-free network (unpaired supervision). Obviously, LIME tends to generate the results with abnormal exposure (e.g., over-exposure appears in the top row, underexposure occurs in the bottom row). RetinexNet tends to bring about the unknown artifacts to influence visual quality. EnlightenGAN produces some inevitable blurs which reduce the visibility of images in detail. In contrast, our method generates more compelling visual performance with substantial details, comfortable exposure and no unwanted components.

- To avoid using the illumination adjustment skills which bring about additional negative gains, we develop a novel SRRP model to simultaneously optimize the illumination and reflectance. In which, the newly-designed self-reinforced fidelity function fully exploits the inherent information of the intermediate reflectance in the optimization procedure towards the desired illumination.
- Thanks to the flexibility of our designed reflectance optimization module with projection, we extend our algorithm to acquire an Enhanced SRRP by introducing a data-driven noise removal network as the projection. In this way, we can successfully eliminate noises/artifacts that are always along with brightness enhancement in some complex real-world scenarios.
- Extensive evaluations on various real-world scenarios fully demonstrate our superiority and practicability in terms of qualitative, quantitative, and execution efficiency against other state-of-the-art techniques. A single image haze removal task is also performed to further indicate the advantage of our designed algorithm.

## II. RELATED WORK

In the past few decades, there emerges a large number of techniques to address the problem of low-light image enhancement. These techniques can be roughly divided into four main categories including S-curve based methods, illumination-based traditional models, illumination-based deep networks, and illumination-free deep networks.

### A. S-curve based Methods

Histogram equalization (HE) [17] is a classical kind of histogram-based method, whose goal is to achieve improve-

ment of exposure level by modifying the histogram distribution. The implementation of HE is simple, but it tends to generate the results with over-exposure and appearance distortion. To address these problems. Different constraints are designed to preserve contrast [18], [19] and weight adjustment [20].

Gamma correction is the most familiar S-curve based method, which is a nonlinear mapping (i.e., power-law function) used to encode and decode luminance in image systems [21]. This method ignores the relationship between pixels, causing the inaccurate of the edge and the loss of details. The work in [22] proposed adopting different S-curve mapping for enhancing each layer decomposed from the input using the bilateral filter. This work achieves the details of preservation but brings the inconsistency of global exposure. In [23], the authors use different S-curve to address subregions generated by segmenting the input. Intuitively, the performance of this work is limited to the quality of graph segmentation, leading to trouble in settling challenging low-light images.

In a word, HE-based methods are useful in images with backgrounds and foregrounds that are both bright or dark. But for non-uniform illuminations, these methods lose efficacy. S-curve based approaches usually bring about color distortion because of lacking the focus on color change.

### B. Illumination-based Traditional Models

Retinex theory states that “sensations of color show a strong correlation with reflectance, even though the amount of visible light reaching the eye depends on the product of reflectance and illumination” [24]. Based on this description, Illumination-based algorithms view Retinex theory as the basic instruction, to design the iterative procedure or network architecture for effectively removing the illumination.

Jobson *et al.* [25] made some basic attempts on how to generate the illumination but obtained an unrealistic appearance in an early stage. However, it generated results with insufficient details and inappropriate exposure. Fu *et al.* [4] built a MAP-based energy model with different prior constraints for different layers, they also proposed a weighted variational model in log-domains for simultaneously estimating illumination and reflectance [5]. The drawbacks of these works lie in the production of ghosting artifacts because of the simplicity of the designed priors. [6] proposed a jointly intrinsic-extrinsic prior model for low-light image enhancement. However, it tended to generate the under-exposure results. The work in [8] first put emphasis on the illumination estimation, which optimized the initial illumination using edge-aware smoothing. Compared with these above-mentioned works, this work achieved the best performance but cannot avoid overexposure during the process. Zhang *et al.* [9] further added extra constraints on the work of [8] to overcome the over-exposure, but it brings the high computational burden. Additionally, because that the estimated reflectance maybe along with noises and artifacts, the paper in [7] developed a denoising-type model to simultaneously estimate the illumination and reflectance. The work in [26] proposed an adaptive low-light image enhancement algorithm by incorporating the multi-scale decomposition and image fusion techniques. Xu *et al.* [27] established a structure and texture aware Retinex model by utilizing exponentiated local derivatives for brightening low-light images. The paper in [10] designed an efficient semi-decoupled way for low-light image enhancement to reduce artifacts generated in the enhanced procedure and improve the computational efficiency.

Actually, a common point of these works lies in that, they all concentrate on how to design the regularization. Therefore, they not only ignore the construction of fidelity but also bring about the computational burden originating from the additional operation (e.g., using Gamma correction as illumination adjustment).

### C. Illumination-based Deep Networks

With the advent of the era of big data, in order to define the desired regularization, it has become a trend to learn the data distribution from massive training pairs. It has achieved prominent accomplishments in many vision-related areas [28], [29], [30]. Data are the chief influencing factor for the development of deep learning in a certain task. Nowadays, because synthetically generating training data has become increasingly convenient, techniques for solving traditional image processing tasks (e.g., super-resolution [31], dehazing [32], deblurring [33]) are almost occupied by deep learning. Different from these tasks, valuable training pairs of low-light image enhancement are difficult to obtain in both the synthetic and real imaging simulation. It limits the development of deep learning in this task.

Chen *et al.* [14] changed the exposure time to build a new dataset (i.e., LOL dataset), and developed a Retinex-based network (named as RetinexNet) to simultaneously estimate the illumination and reflectance. They not only performed an illumination adjustment network to correct the illumination

but also presented a restoration network to further optimize the obtained reflectance. LightenNet [34] was designed based on convolutional neural network for weakly illuminated image enhancement. This work generated training pairs based on the Retinex theory. Wang *et al.* [35] generated low-light pairs based on the strategy presented in MIT-Adobe FiveK [36]. This work used the network architecture described in the work [37] and three different loss functions were defined to estimate the illumination, the enhanced result was further obtained by performing the Retinex theory. Yang *et al.* [38] proposed a semi-supervised learning framework by introducing the coarse-to-fine recursive band representation. The work in [39] constructed a Retinex-inspired deep network to improve lightness and remove degradation for low-light images. It also built a learned mapping function to flexibly adjust light levels.

Unfortunately, the above-mentioned works heavily depend on the paired datasets which are obtained by manually retouching or adjusting. They are difficult to satisfy the actual demand, especially in complex real-world scenarios that present different distribution forms with the training dataset.

### D. Illumination-free Deep Networks

Utilizing the strong learning ability of the network to build the mapping is an intuitive idea. In [37], a new network architecture (HDRNet) based on bilateral grid and affine transformation was proposed for real-time image enhancement. The training pairs were obtained from the well-known MIT-Adobe FiveK [36] which generated the labels by expert-retouched. [40] proposed an autoencoder-based network and trained this network by training pairs based on Gamma Correction. The work in [41] generated a paired dataset of raw by considering different exposure time, and proposed an end-to-end fully convolutional network to handle the low-light image enhancement. Cai *et al.* [42] constructed a multi-exposure dataset and trained a network under the training labels, which were obtained by using existing techniques. Considering the difficulty and inaccuracy of data acquisition, [15] established an unsupervised generative adversarial network, dubbed EnlightenGAN. Because of the ability of GAN, this work does not need to generate a training dataset with low/normal-light. The work in [43] proposed a deep stacked Laplacian restorer to enhance the low-light images from the global and local views. A two-branch fusion network was developed in [44] to brighten the low-light images by an introduced generation-and-fusion strategy. Xu *et al.* [45] built a frequency-based decomposition-and-enhancement framework with attention-to-context encoding for noise suppression and detail enhancement for low-light images. ZeroDCE [46] developed a zero-reference algorithm by designing an image-specific curve that approximates pixel-wise and higher-order curves.

We know that the physical principle reflects the general regular to cater to most of the scenes. While illumination-free works only concentrated on the establishment of the mapping by observations or data. They ignored the usage and modeling of physical principles. Therefore, they cannot effectively handle most of the low-light scenarios.

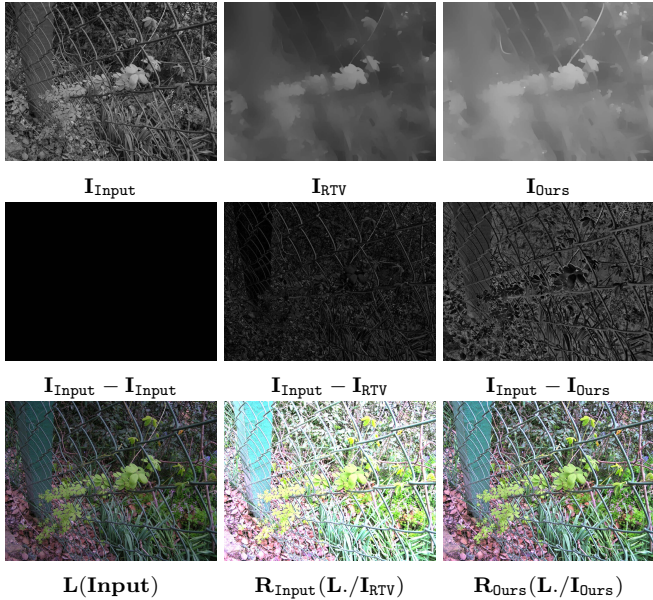


Fig. 3. Visual comparison of different components. These results are generated by directly using RTV and our proposed SRRP. In which,  $I_{Input}$  is the v-channel of the input after the “RGB2HSV” conversion.

### III. THE PROPOSED ALGORITHM

In this section, we clearly describe our motivation at first. We then develop a novel self-reinforced Retinex projection model consists of illumination and reflectance optimization modules. We derive a solving scheme to address this proposed model. Also, an enhanced version of our proposed model is provided to effectively handle the case that noises/artifacts occur in the process of low-light image enhancement.

#### A. Motivation

Retinex theory [24] describes the phenomenon of human color vision. It can be expressed as  $\mathbf{L} = \mathbf{I} \odot \mathbf{R}$ , where  $\mathbf{L} \in \mathbb{R}^{H \times W}$  is the low-light input,  $\mathbf{I} \in \mathbb{R}^{H \times W}$  is the illumination layer which represents the back/front-lighting,  $\mathbf{R} \in \mathbb{R}^{H \times W}$  is the reflectance layer which is the intrinsic structure after removing the spatial-varying illumination layer.

Actually, most existing illumination-based works attach importance to the illumination estimation. A widely-used illumination estimation model is the classical image smoothing model [47], [48], [16]. Edge-preserving smoothness [5], [8], [9] is the most familiar way for defining the smoothing model. Relative Total Variation (RTV) [16] is a well-known image smoothing algorithm and commonly used in existing low-light image enhancement work ([8], [9], [49]).

In Figure 3, we used RTV to estimate the illumination and obtained the derived reflectance based on the Retinex theory. It can be readily observed that over-exposure occurs in the reflectance estimated by RTV (i.e.,  $R_{RTV}$ ). It is because RTV realized the smoothness by changing the value distribution of adjacent pixels, according to the sparsity constraint of the image gradient. As shown in the middle row of Figure 3, the difference (i.e.,  $I_{Input} - I_{RTV}$ ) of estimated illumination between the input and RTV existed in some tiny pixel values. What’s more, in Figure 4, we plotted histogram distributions of the

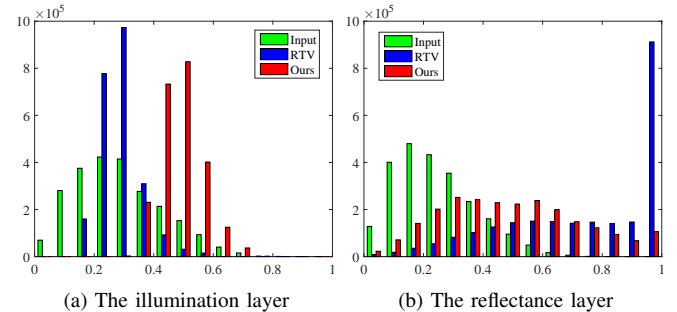


Fig. 4. The histogram distribution of different components. These results come from Figure 3.

illumination and reflectance layers. In the subfigure (b), we can see that many values of RTV are the maximum pixel value, and it can further demonstrate the cause of over-exposure.

As shown in Figure 1, the illumination adjustment operator is a compensation for the illumination estimation model. In other words, the capacity of the existing illumination estimation model is not enough to estimate an accurate illumination. In which, the smoothed regularization can exactly cater to our desired property of the illumination, so the possible reason turns to the neglect of how to design the effective fidelity.

#### B. Self-Reinforced Retinex Projection Model

Our defined Self-Reinforced Retinex Projection (SRRP) model contains two parts: illumination and reflectance optimization modules. In the following, we first fix the reflectance to design the illumination optimization module, then fix the illumination to define the reflectance optimization module.

**Illumination Optimization Module.** We know that the gradient-based smooth constraint is essential and indispensable. Actually, the fidelity term acts on the image domain, and predominates the output. So we change the form of data fidelity to improve the capacity of the model. We define a new self-reinforced function to act on the reflectance as the input of the illumination optimization model. We also define a weighted  $\ell_2$ -regularization as regularization. The formulation can be described as

$$\mathbf{I}^{t+1} = \arg \min_{\mathbf{I}} \frac{1}{2} \|\mathbf{I} - \mathcal{D}(\mathbf{R}^t)\|_2^2 + \frac{\lambda}{2} \varphi(\nabla \mathbf{I}), \quad (1)$$

where  $t = 1, \dots, T$  is the iteration number.  $\lambda$  is a positive weighting parameter. We empirically set it as 0.1.  $\mathcal{D}(\cdot)$  is the self-reinforced function described as

$$\mathcal{D}(\mathbf{R}^t(x, y)) = \max_{i=\{0,1\}} \left( \max_{j=\{0,1\}} (\mathbf{R}^t(x+i, y+j)) \right) + c, \quad (2)$$

where  $(x, y)$  denotes the pixel position.  $c$  is the exposure control constant<sup>1</sup>. We presented some examples to analyze the effect of self-reinforced function in Figure 5. We can see that  $\mathcal{D}(Input)$  strengthens the structural expression in the edge and outline of the Input. The difference between them is shown in the third column (i.e.,  $\mathcal{D}(Input) - Input$ ), it can further verify the effect of self-reinforced function. In this way, we

<sup>1</sup>We will make the elaborated analyses to illustrate the necessity and effectiveness of this operator in Sec. IV.

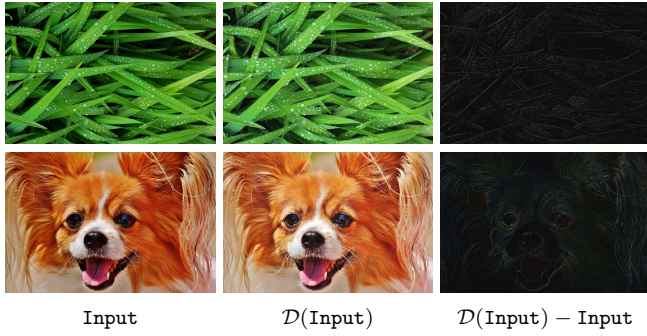


Fig. 5. Visual comparison of self-reinforced function  $D(\cdot)$ . Best viewed full screen to see details.

successfully enlarge the value distribution of the original input by utilizing the intrinsic information of the original input rather than depend on the value mapping (e.g., Gamma Correction), which damages the structural characterization.

$\varphi(\cdot)$  is the spatially smooth constraint based on  $\ell_2$ -norm, whose concrete form can be formulated as

$$\varphi(\nabla \mathbf{I}(x, y)) = \sum_{i \in \{h, v\}} \mathcal{W}_i(\mathbf{L}(x, y)) (\nabla_i \mathbf{I}(x, y))^2, \quad (3)$$

where  $(x, y)$  indicates the spatial location of the pixel,  $\nabla_h$  and  $\nabla_v$  denote the horizontal and vertical gradient, respectively.  $\mathcal{W}_i(\cdot)$  is a weight function, presented as

$$\mathcal{W}_i(\mathbf{L}(x, y)) = \frac{\mathbf{G}_i(\mathbf{L}(x, y))}{|\nabla_i \mathbf{L}(x, y)| + \varepsilon}, i \in \{h, v\}, \quad (4)$$

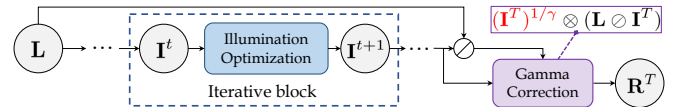
where  $\mathbf{G}_i(\mathbf{L}(x, y)) = \mathcal{G}_\delta \otimes \frac{1}{|\mathcal{G}_\delta \otimes \nabla_i \mathbf{L}(x, y)|}$ ,  $\mathcal{G}$  is the Gaussian filter with the standard deviation  $\delta$ .  $\otimes$  denotes the convolution operator.  $\varepsilon$  is a small constant to avoid division by zero. Our weight function is fixed in the whole iteration and needs to be calculated once at the initial stage. Actually, our defined  $\ell_2$ -regularization is a simplified version of the RTV. Instead of the weighting parameter related to the immediate output which is adopted in RTV, we adopt a fixed weighting parameter which is related to the low-light input. We can reformulate the regularization of RTV as our presented  $\ell_2$ -regularization with a fixed weighting coefficient. It can reduce the computational burden. As shown in Figure 3, our designed illumination optimization module generates a task-related illumination, resulting in a more natural enhanced result without overexposure.

As for solving the illumination optimization module, we used the strategy described in [50] based on 1D Fast Global Smoother to solve Eq. (1). In this way, we can ensure a fast inference to obtain the desired illumination.

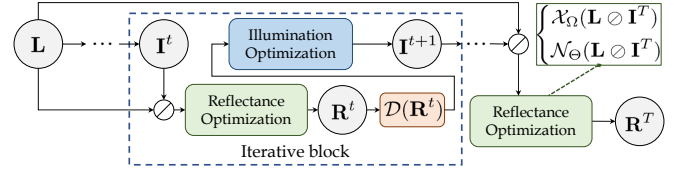
**Reflectance Optimization Module.** After obtaining the illumination, we build the reflectance optimization module to obtain the reflectance, described as the following formulation

$$\mathbf{R}^{t+1} = \arg \min_{\mathbf{R}} \frac{1}{2} \|\mathbf{L} - \mathbf{R} \odot \mathbf{I}^{t+1}\|^2, \quad s.t. \quad \mathbf{R} \in \Omega, \quad (5)$$

where  $\Omega$  is the feasible constraint. Considering the intrinsic range of the image, here we define  $\Omega = [0, 1]$ . Actually,  $\Omega$  is flexible so that it can be defined as the more complex forms to adapt some challenging real-world scenarios. We will make an extension in the following to verify this point.



(a) The computational flow of existing works, e.g., LIME [8], PBS [19].



(b) Our computational flow.

Fig. 6. Comparison of computational flow. Our reflectance optimization contains two forms toward different scenarios. Because of inappropriate propagation occurs in the iterative block of (a), the additional illumination adjustment operation (i.e., Gamma correction) is needed to suppress the overexposure. By contrast, our method does not need any attached operations that are irrelevant to the solving goal.

For the reflectance optimization module, we can directly solve it by the following formulation

$$\mathbf{R}^{t+1}(x, y) = \mathcal{X}_\Omega \left( \frac{\mathbf{L}(x, y)}{\mathbf{I}^{t+1}(x, y)} \right), \quad (6)$$

where  $\mathcal{X}_\Omega$  denotes the projection about  $\Omega$ .

### C. Enhanced Self-Reinforced Retinex Projection Model

In many real-world scenarios, noises are always generated in the process of low-light image enhancement. Thus it is essential to perform the process of noises removal. Thanks to the flexibility of our proposed self-reinforced Retinex projection model, we can easily incorporate the noise removal process. To be specific,  $\Omega$  is the solution space of the denoising network, then we can obtain Eq. (6) as the following form

$$\mathbf{R}^{t+1}(x, y) = \mathcal{N}_\Theta \left( \frac{\mathbf{L}(x, y)}{\mathbf{I}^{t+1}(x, y)} \right), \quad (7)$$

where  $\mathcal{N}$  is the denoising network for real-world scenarios,  $\Theta$  is the network parameters. Here we adopt an advanced network, i.e., CBDNet [51]. For CBDNet, we directly use its pre-trained model, rather than retraining it using low-light data. In other words, CBDNet only executes the task of noises removal to improve visual quality. In order to respond to more complex cases, we can enhance the ability of SRRP to obtain an Enhanced SRRP (ESRRP). The experimental results will be demonstrated on Sec. IV.

Until now, we have introduced all details of our method. Figure 6 shows the difference in computational flow between our proposed method and the mainstream low-light image enhancement method. We successfully avoid introducing Gamma correction to overcome the overexposure brought by the inappropriate propagation in (a), and retain the excellent smoothness derived from the illumination optimization.

## IV. EXPERIMENTAL RESULTS

In this section, we made a range of experiments to evaluate the proposed algorithm. Compared methods, benchmarks and metrics were first introduced to perform the experimental settings. A group of visual comparison in terms of decomposed

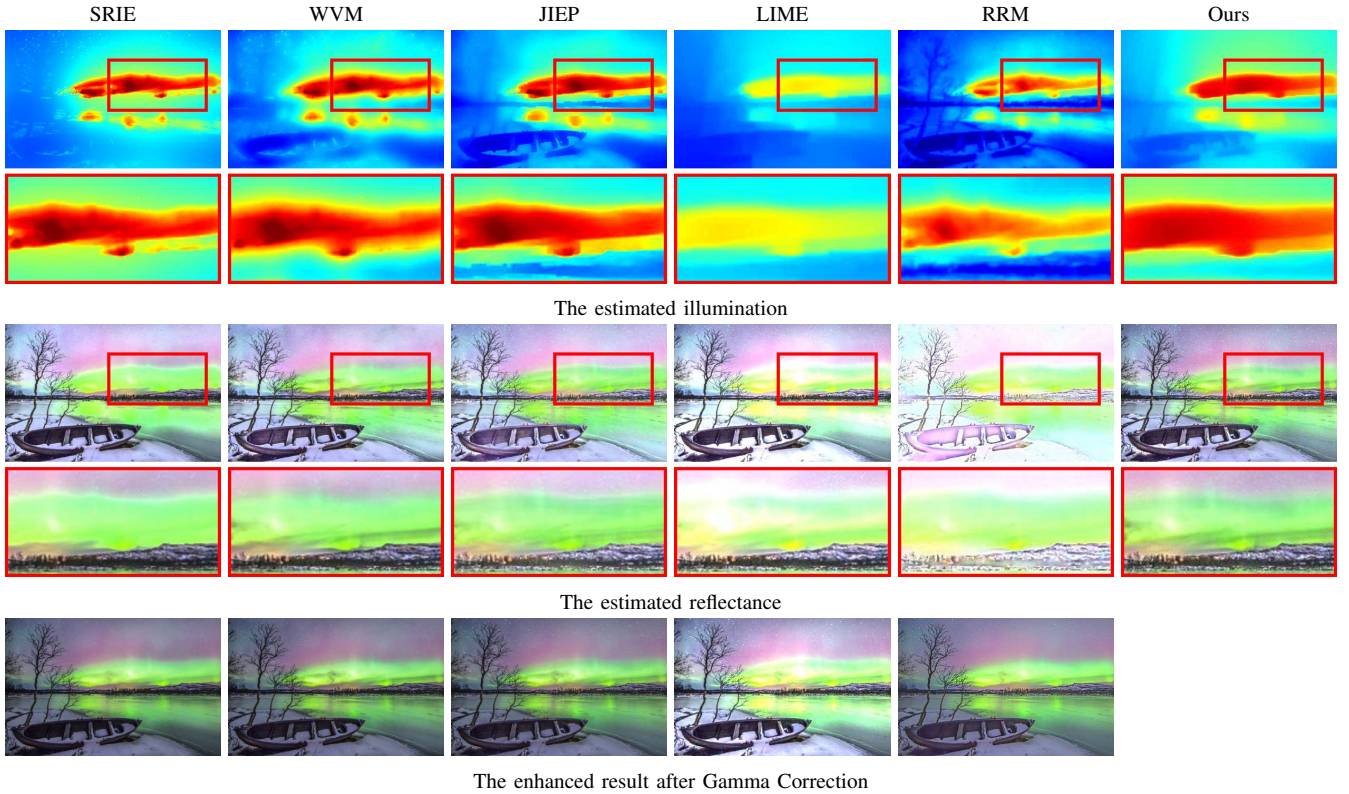


Fig. 7. Visual comparison of the decomposition components and the enhanced results. Notice that the reflectance of our method is exactly the final enhanced result. However, other works all need to perform the *Gamma Correction* as the post-processing to overcome the over-exposure. As fully utilizing the inherent structural information, we can accurately recover more details and textures in the reflectance without over-exposure.

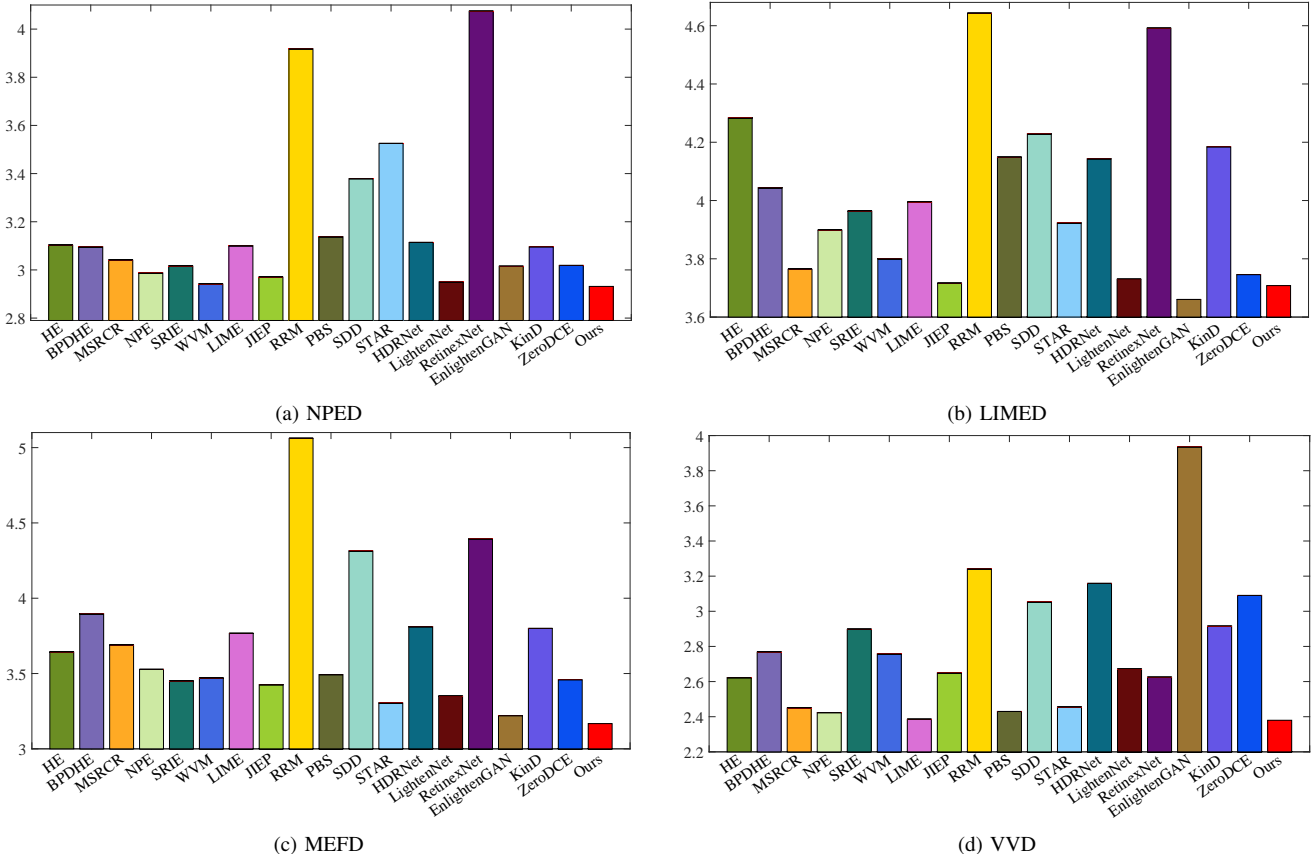


Fig. 8. Quantitative performance (i.e., NIQE, lower is better) among fourteen state-of-the-art methods and our SRRP on four benchmarks.



Fig. 9. Visual comparison on a low-light outdoor image.

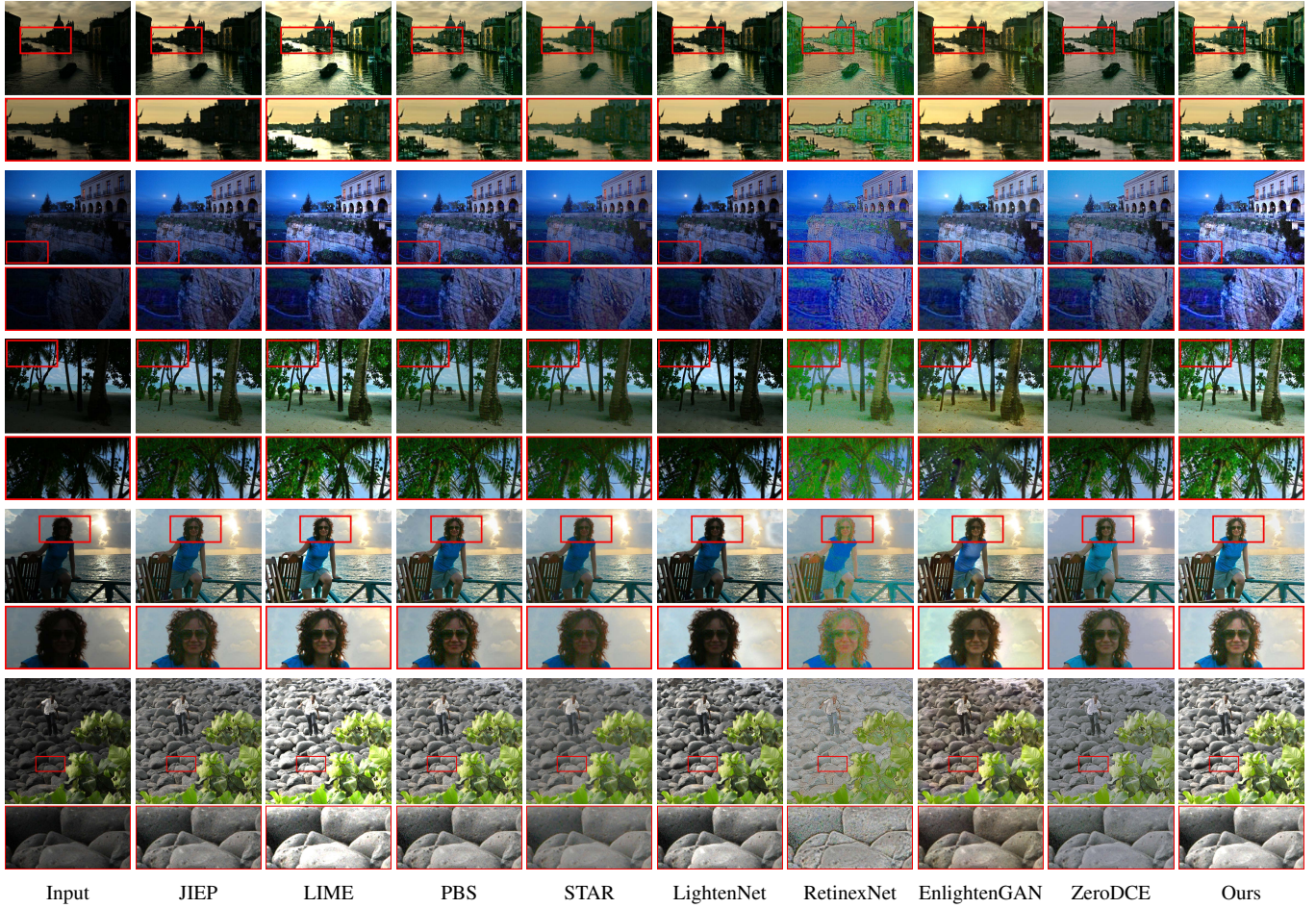


Fig. 10. More visual comparison of low-light image enhancement.

TABLE I

PSNR/SSIM RESULTS ON 100 TESTING IMAGES RANDOMLY SAMPLED FROM LOL DATASET AMONG DIFFERENT STATE-OF-THE-ART METHODS.

| Metrics | SRIE    | WVM     | LIME    | JIEP    | RRM     | PBS     | SDD     | STAR    | RetinexNet | EnlightenGAN  | KinD    | ZeroDCE | Ours           |
|---------|---------|---------|---------|---------|---------|---------|---------|---------|------------|---------------|---------|---------|----------------|
| PSNR    | 15.5117 | 14.7596 | 16.8588 | 14.9908 | 18.0869 | 18.5788 | 17.1544 | 16.6603 | 19.1979    | 20.1848       | 19.3623 | 19.2049 | <b>20.9405</b> |
| SSIM    | 0.6320  | 0.6089  | 0.7592  | 0.6456  | 0.7727  | 0.7978  | 0.7275  | 0.7135  | 0.8091     | <b>0.8436</b> | 0.8301  | 0.7752  | 0.8071         |

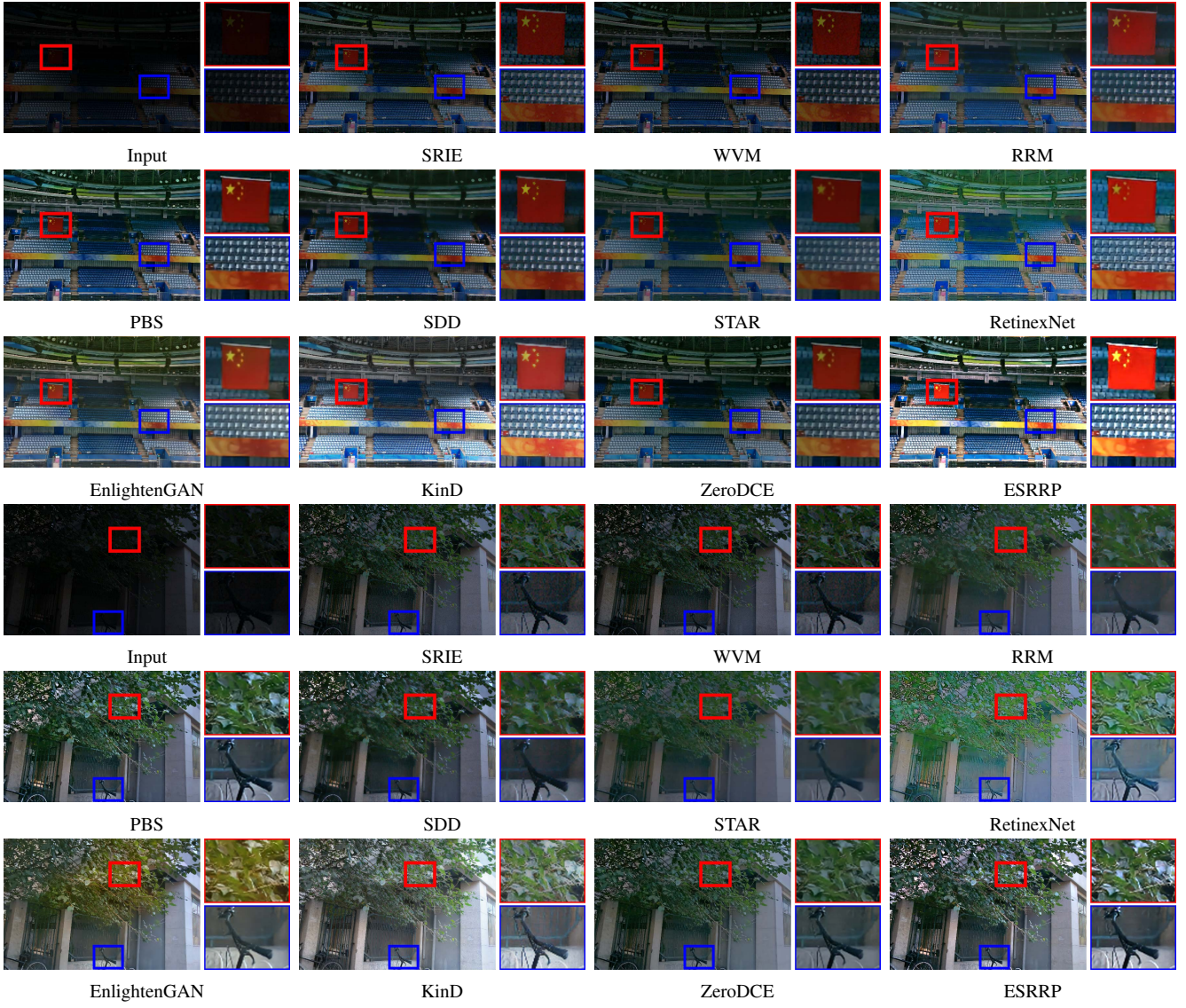


Fig. 11. Visual comparison on two testing images from LOL dataset. The noises/artifacts are generated in the procedure of low-light enhancement. We introduce the additional denoising network CBDNet [51] as the post-processing in all of the compared methods (except RRM and KinD, they also consider the noise modeling). Similarly, we introduce CBDNet in the reflectance optimization module to obtain our ESRRP.

components was conducted to verify our advantage. Qualitative and quantitative comparisons among fourteen state-of-the-art approaches on four standard benchmarks were further presented. We compared the running times on three scales of images to reflect our practicability. Plenty of algorithmic evaluations, including effects of denoising operation, analyses of self-reinforced function and convergence behavior were also performed. Finally, we tested our SRRP on image dehazing to verify our scalability. All experiments were conducted on a PC with an Intel Core i7-8700 CPU at 3.70GHz, 32 GB RAM and an NVIDIA GeForce GTX 1080 Ti 11 GB GPU.

#### A. Compared Methods, Benchmarks and Metrics

**Compared Methods.** An amount of existing low-light image enhancement methods are considered for comparison, including several illumination-based methods (i.e., M-SRCR [52], SRIE [4], WVM [5], LIME [8], JIEP [6], R-RM [7], PBS [9], STAR [27], SDD [10], LightenNet [34],

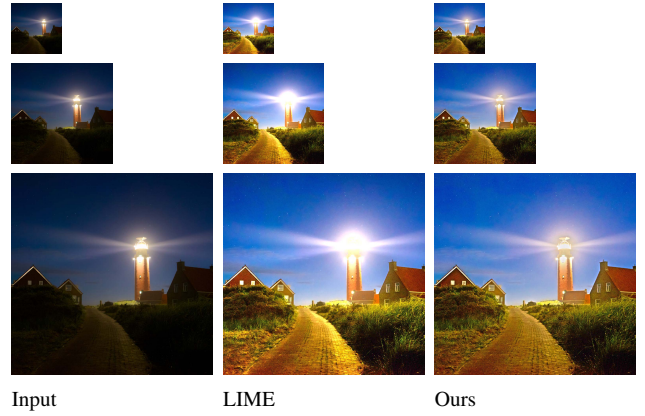


Fig. 12. Visual comparison among our method and LIME on three images with different sizes.

RetinexNet [14], KinD [39]), illumination-free methods, (i.e,

TABLE II  
COMPARISON OF RUNNING TIME (SECONDS).

| Image Size | NPEA  | SRIE | WVM   | LIME | JIEP | RRM   | PBS   | SDD   | STAR | HDRNet | LightenNet | RetinexNet | EnlightenGAN | KinD | ZeroDCE | SRRP        |
|------------|-------|------|-------|------|------|-------|-------|-------|------|--------|------------|------------|--------------|------|---------|-------------|
| 256×256    | 2.01  | 0.44 | 2.11  | 0.17 | 0.49 | 2.41  | 1.39  | 0.83  | 0.19 | 4.46   | 0.77       | 2.29       | 0.59         | 0.06 | 0.04    | <b>0.01</b> |
| 512×512    | 8.11  | 0.48 | 7.03  | 0.21 | 2.42 | 13.20 | 3.91  | 4.72  | 0.83 | 5.83   | 2.66       | 4.28       | 0.62         | 0.17 | 0.11    | <b>0.05</b> |
| 1024×1024  | 31.03 | 1.82 | 26.77 | 0.57 | 9.36 | 56.59 | 15.19 | 25.38 | 3.36 | 7.42   | 10.27      | 12.09      | 0.79         | 0.56 | 0.43    | <b>0.17</b> |

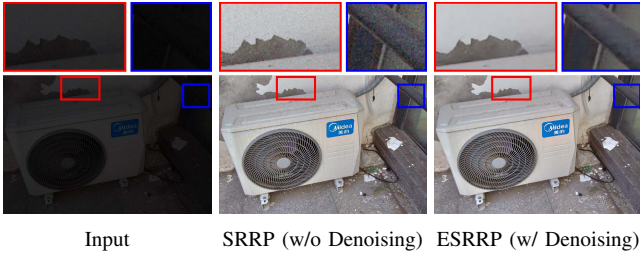


Fig. 13. Effects of the denoising operation.

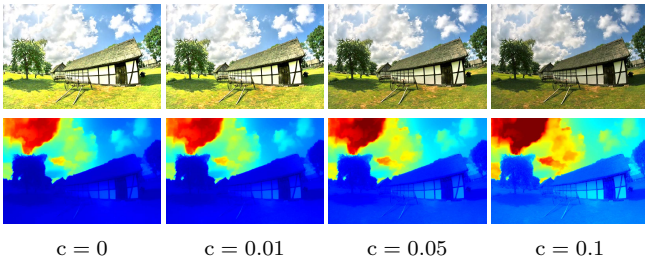


Fig. 14. Effect of different  $c$ . **Top** and **Bottom** represent the final enhanced results and the estimated illumination layers among different methods.

HE [17], BPDHE [19], NPE [53], HDRNet [37], EnlightenGAN [15], ZeroDCE [46]).

As for all of the compared methods, we used their default settings of parameters. To be concrete, for those non-learning methods (including MSRCE, SRIE, WVM, LIME, RRM, PBS, STAR, SDD, HE, BPDHE, NPE), we directly obtained their testing results by using the provided settings in source codes. As for learning-based methods (including LightenNet, RetinexNet, KinD, HDRNet, EnlightenGAN, ZeroDCE), we used their pre-trained models. These learning-based methods obtained their network models by using completely different datasets. But we would like to emphasize that the above-mentioned benchmarks are not contained in their training sets. That is to say, both non-learning and learning compared approaches are impartially tested on these unknown datasets.

**Benchmarks and Metrics.** We took four well-known benchmarks into account, including NPED [53] which consists of 130 low-light images in different natural scenarios, LIMED [8] which is composed of 10 nighttime low-light images, Mefd [54] which contains 17 indoor and outdoor low-light images, VVD<sup>2</sup> [55] which contains 23 images with evident darkness in the foreground. Natural Image Quality Evaluator (NIQE) [56] is the most common qualitative measure in the low-light image enhancement task [5], [8], [15]. This metric indicates the naturalness of a single image.

<sup>2</sup><https://sites.google.com/site/vonikakis/datasets>

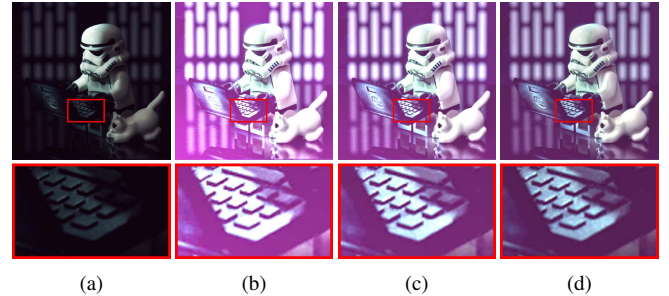


Fig. 15. Visual comparison about the position of self-reinforced function. (a) low-light input; (b) self-reinforced function ( $c = 0$ ) is used for initialization of the illumination in the beginning; (c) self-reinforced function ( $c = 0.05$ ) is used for initialization of illumination in the beginning; (d) self-reinforced function ( $c = 0.05$ ) is used in the each iteration.

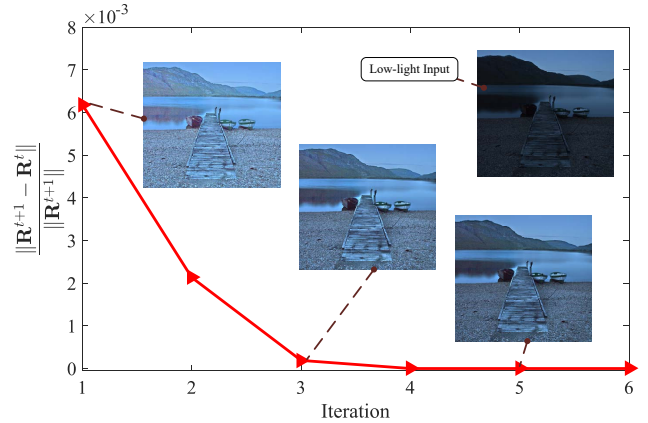


Fig. 16. The convergence curve of our proposed algorithm.

Notice that the lower value of NIQE represents a higher image quality. Further, we evaluated the enhancement on 100 testing images from LOL dataset [14] that contained visible noises in the enhanced procedure. To suppress noises, we directly utilized the pre-trained denoising network CBDNet as the denoising module and performed it in all the compared methods to ensure fairness. We adopted PSNR and SSIM to evaluate the performance. In addition, we performed the task of single image haze removal to verify our superiority on the RESIDE dataset [57] by comparing with state-of-the-art dehazing works.

#### B. Visual Comparison of Decomposed Components

We conducted an experiment to show the visual comparison of the estimated components in Figure 7. We selected five representative illumination-based methods including SRIE [4], WVM [5], JIEP [6], LIME [8], and RRM [7]. Obviously, the reflectance layers of all compared methods are over-

TABLE III  
IMAGE DEHAZING RESULTS ON RESIDE DATASET [57].

| Metrics | DCP [58] | DehazeNet [59] | EPDN [60] | GFN [61] | FFANet [62] | PhysicGAN [63] | RefineDNet [64] | MSCNN [65] | Ours           |
|---------|----------|----------------|-----------|----------|-------------|----------------|-----------------|------------|----------------|
| PSNR    | 16.0609  | 18.5467        | 21.6702   | 22.9753  | 20.7591     | 20.3277        | 21.0321         | 18.6618    | <b>23.5210</b> |
| SSIM    | 0.8370   | 0.8182         | 0.8236    | 0.8828   | 0.9004      | 0.6749         | 0.8807          | 0.8172     | <b>0.9213</b>  |

Fig. 17. Visual comparison of single image haze removal on RESIDE dataset.

exposure (as demonstrated in zoomed-in regions) because of the inappropriate illumination estimation model. As far as the final enhanced results, Gamma Correction has powerful impacts on the over-smooth illumination. Compared with them, our method generates the illumination with an appropriate smooth level, and the estimated reflectance is exactly the final enhanced result. In a word, our SRRP achieves a more ideal and natural performance in terms of all estimated components against compared methods.

### C. Evaluation on Regular Low-light Scenarios

Figure 8 reported the quantitative results among eighteen state-of-the-art methods and our method on four benchmarks. Obviously, our method reached the lowest NIQE values of all benchmarks in most cases, which adequately demonstrates the excellent naturalness of the enhanced results obtained by our proposed SRRP. Figure 9 showed the visual comparison among our method and some advanced illumination-based (including JIEP, LIME, RRM, PBS, SDD, STAR, Lighten-Net, RetinexNet, KinD), illumination-free methods (including HDRNet, EnlightenGAN, ZeroDCE) on an example sampled from [9]. Obviously, illumination-based traditional methods uniformly generate more natural results than network-based methods. However, the level of exposure and structural expression of illumination-based traditional approaches exist conspicuous deficiency. ‘Paired training based methods (i.e., HDRNet, LightenNet, RetinexNet, KinD) are limited to training data, leading the unnatural performance with inappropriate

exposure and color distortion. Notice that EnlightenGAN and ZeroDCE were trained without low/normal-light image pairs, the absence of physical knowledge brought about some unknown blurs and artifacts. Compared with them, we possessed the best visual expression with appropriate exposure and sufficient details. More visual comparisons (especially the zoomed-in regions) were conducted in Figure 10 to provide more convincing evidence for verifying our superiority.

### D. Evaluation on Complex Low-light Scenarios

Further, we considered the challenging scenarios that contained the unknown noises after enhancement. We made the evaluation on the widely-adopted LOL dataset that contained 100 testing images. Notice that the compared methods RetinexNet and KinD were trained by using the training samples from the LOL dataset. As shown in Table I, it can be easily seen that our method realized the competitive numerical scores. We also provided visual comparisons of indoor and outdoor scenarios in Figure 11. By comparison, our method obtained prominent visual performance both in details recovery, exposure correction, and noise removal. All of the illumination-based approaches were still hard to present proper lightness and adequate details, especially RRM, which lost almost all the details in the zoomed-in regions. The result of RetinexNet had a prominent promotion of lightness, but it looked unnatural. Other methods were difficult to recover clear details and correctly display the exposure. In contrast, our exposure degree and detail expression are remarkable.

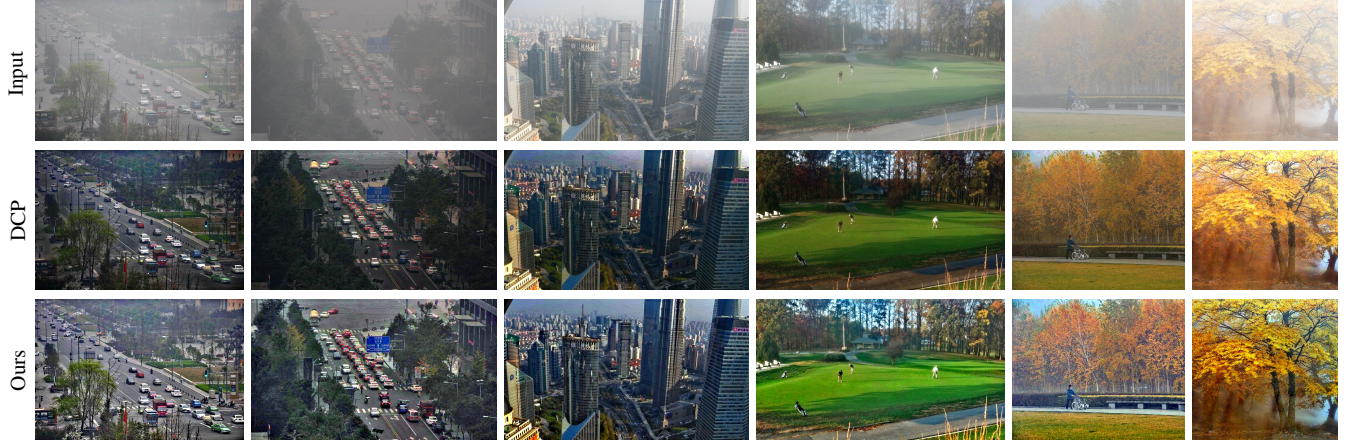


Fig. 18. Visual comparison among DCP [58] and our method on single image haze removal.

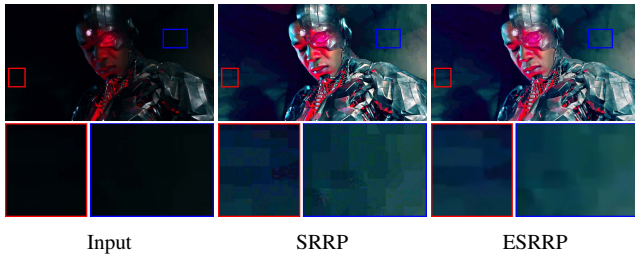


Fig. 19. A failure example. Although denoising was considered, the blocking artifacts appeared in the enhanced results.

#### E. Running Time

To evaluate the execution efficiency, for example, we generated different sizes of images including  $256 \times 256$ ,  $512 \times 512$ , and  $1024 \times 1024$ . As demonstrated in Table II, we can easily see that our SRRP achieved the conspicuous performance in all cases, which fully indicates our practicability. We also compared the visual performance of our SRRP and the second fastest method (i.e., LIME [8]). As shown in Figure 12. It is obvious that our results are more stable and outstanding than the state-of-the-art method LIME in all cases.

#### F. Effects of Denoising

Actually, we designed two versions for our proposed algorithm to deal with different scenarios. The core improvement lay in the introduction of the denoising network. Here we demonstrated the visual comparison among them in Figure 13. We can observe that the denoising operation was essential to remove visible noises to further boost the visual performance, especially in the zoomed-in regions. It also verified the necessity of introducing the denoising process.

#### G. Effects of Self-Reinforced Function

As described in Sec. III, we design the self-reinforced function to inhibit the issues (e.g., over-exposure) generated in the illumination optimization module. Figure 15 illustrated the reason why this function is a prerequisite in each iteration of the whole solving procedure. Especially in zoomed-in regions, it is apparent that using this operator once causes

the over-exposure. However, our strategy (i.e., executing this operator in each iteration) generates preferable performance with high contrast and abundant details. We further analyzed the influences of different exposure control constant for the final enhanced result. As shown in Figure 14, along with the increase of  $c$ , the estimated illumination tends to generate more details, which looks like non-smooth. It further brings about a darker results after the enhancement process. So we empirically set  $c$  from the range of  $[0.01, 0.1]$ , and we defined it as 0.05 in general.

#### H. Convergence Evaluation

We plotted the convergence curve of our proposed algorithm in Figure 16. We used the relative error in terms of the final reflectance. Some immediate results are also shown in this figure. It is easy to find that our SRRP generally possesses fast convergence, 5 iterations specifically. This is also one of the reasons that our SRRP is the fastest among all existing works. Additionally, from the change of visual expression, our first enhanced result is the brightest among existing works in the whole process. It is also one of the key reasons why our proposed algorithm possesses fast convergence.

#### I. Single Image Haze Removal

Following the duality between Retinex and image dehazing described in [66], we tested the single image haze removal task by utilizing our proposed SRRP quantitatively and qualitatively. We compared our method with a classical and famous method Dark Channel Prior (DCP) [58], seven recently-proposed learning-based approaches that contained DehazeNet [59], EPDN [60], GFN [61], FFANet [62], Physic-GAN [63], RefineDNet [64], and MSCNN [65]. Table III reported the numerical scores on the synthetic HSTS benchmark from the RESIDE dataset [57]. It can be easily observed that our method was significantly superior to others. Moreover, we showed the visual comparison in Figure 17. As presented in the zoomed-in regions, all the compared methods failed to recover the structural information and perform the appropriate exposure. Fortunately, our method overcame these issues to present the better visual effects. Additionally, we also provided

visual comparisons among DCP and ours on real-world scenarios. Obviously, our algorithm can effectively remove haze and perform accurate color expression. The above evaluation on single image haze removal manifests our scalability.

### J. Limitations

Figure 19 demonstrated a failure example of using our proposed algorithm. Although we obtained a significant brightness improvement, the blocking artifacts became inevitable degraded factors both in SRRP and ESRRP. It is because of transform coding takes effect in imaging. Fortunately, we can follow the built process of ESRRP to introduce a blocking artifacts removal technique to obtain our wanted results. We will realize it in our future work.

## V. CONCLUDING REMARKS

In this work, we developed a novel Self-Reinforced Retinex Projection (SRRP) model to avoid breaking down the favorable smoothness property by utilizing the illumination adjustment (e.g., Gamma Correction) as the post-processing. Our SR-RP contains the illumination and reflectance optimization modules so as to simultaneously optimize the illumination and reflectance. We also achieved an enhanced version by integrating the data driven denoising network to effectively reduce the appearance of noises/artifacts in the procedure of enhancement. We made extensive assessments and analytical experiments to indicate our superiority and effectiveness.

## REFERENCES

- [1] B. Huang, T. Xu, S. Jiang, Y. Chen, and Y. Bai, “Robust visual tracking via constrained multi-kernel correlation filters,” *IEEE TMM*, vol. 22, no. 11, pp. 2820–2832, 2020.
- [2] G. Varol, I. Laptev, and C. Schmid, “Long-term temporal convolutions for action recognition,” *IEEE TPAMI*, vol. 40, no. 6, pp. 1510–1517, 2018.
- [3] J. Li, X. Liang, J. Li, Y. Wei, T. Xu, J. Feng, and S. Yan, “Multistage object detection with group recursive learning,” *IEEE TMM*, vol. 20, no. 7, pp. 1645–1655, 2017.
- [4] X. Fu, Y. Liao, D. Zeng, Y. Huang, X.-P. Zhang, and X. Ding, “A probabilistic method for image enhancement with simultaneous illumination and reflectance estimation,” *IEEE TIP*, vol. 24, no. 12, pp. 4965–4977, 2015.
- [5] X. Fu, D. Zeng, Y. Huang, X.-P. Zhang, and X. Ding, “A weighted variational model for simultaneous reflectance and illumination estimation,” in *CVPR*, 2016.
- [6] B. Cai, X. Xu, K. Guo, K. Jia, B. Hu, and D. Tao, “A joint intrinsic-extrinsic prior model for retinex,” in *CVPR*, 2017.
- [7] M. Li, J. Liu, W. Yang, X. Sun, and Z. Guo, “Structure-revealing low-light image enhancement via robust retinex model,” *IEEE TIP*, vol. 27, no. 6, pp. 2828–2841, 2018.
- [8] X. Guo, Y. Li, and H. Ling, “Lime: Low-light image enhancement via illumination map estimation,” *IEEE TIP*, vol. 26, no. 2, pp. 982–993, 2017.
- [9] Q. Zhang, Y. Nie, L. Zhu, C. Xiao, and W.-S. Zheng, “Enhancing underexposed photos using perceptually bidirectional similarity,” *IEEE TMM*, 2020.
- [10] S. Hao, X. Han, Y. Guo, X. Xu, and M. Wang, “Low-light image enhancement with semi-decoupled decomposition,” *IEEE TMM*, 2020.
- [11] L. Ma, R. Liu, J. Zhang, X. Fan, and Z. Luo, “Learning deep context-sensitive decomposition for low-light image enhancement,” *IEEE TNNLS*, 2021.
- [12] R. Liu, L. Ma, J. Zhang, X. Fan, and Z. Luo, “Retinex-inspired unrolling with cooperative prior architecture search for low-light image enhancement,” in *CVPR*, 2021, pp. 10561–10570.
- [13] R. Liu, L. Ma, Y. Zhang, X. Fan, and Z. Luo, “Underexposed image correction via hybrid priors navigated deep propagation,” *IEEE TNNLS*, 2021.
- [14] C. Wei, W. Wang, W. Yang, and J. Liu, “Deep retinex decomposition for low-light enhancement,” in *BMVC*, 2018.
- [15] Y. Jiang, X. Gong, D. Liu, Y. Cheng, C. Fang, X. Shen, J. Yang, P. Zhou, and Z. Wang, “Enlightengan: Deep light enhancement without paired supervision,” *IEEE TIP*, vol. 30, pp. 2340–2349, 2021.
- [16] L. Xu, Q. Yan, Y. Xia, and J. Jia, “Structure extraction from texture via relative total variation,” *ACM TOG*, 2012.
- [17] H. Cheng and X. Shi, “A simple and effective histogram equalization approach to image enhancement,” *DSP*, vol. 14, no. 2, pp. 158–170, 2004.
- [18] C. Wang and Z. Ye, “Brightness preserving hisram equalization with maximum entropy: a variational perspective,” *IEEE TCE*, vol. 51, no. 4, pp. 1326–1334, 2005.
- [19] D. Sheet, H. Garud, A. Suveer, M. Mahadevappa, and J. Chatterjee, “Brightness preserving dynamic fuzzy histogram equalization,” *IEEE TCE*, vol. 56, no. 4, 2010.
- [20] S. H. Yun, H. K. Jin, and S. Kim, “Contrast enhancement using a weighted histogram equalization,” in *IEEE ICCE*, vol. 10, no. 11, 2011, pp. 203–204.
- [21] C. Poynton, *Digital video and HD: Algorithms and Interfaces*, 2012.
- [22] E. P. Bennett and L. McMillan, “Video enhancement using per-pixel virtual exposures,” *ACM TOG*, vol. 24, no. 3, pp. 845–852, 2005.
- [23] L. Yuan and J. Sun, “Automatic exposure correction of consumer photographs,” in *ECCV*. Springer, 2012, pp. 771–785.
- [24] E. H. Land and J. J. McCann, “Lightness and retinex theory,” *Journal of the Optical Society of America*, 1971.
- [25] D. J. Jobson, Z.-u. Rahman, and G. A. Woodell, “A multiscale retinex for bridging the gap between color images and the human observation of scenes,” *IEEE TIP*, vol. 6, no. 7, pp. 965–976, 1997.
- [26] W. Wang, Z. Chen, X. Yuan, and X. Wu, “Adaptive image enhancement method for correcting low-illumination images,” *Information Sciences*, vol. 496, pp. 25–41, 2019.
- [27] J. Xu, Y. Hou, D. Ren, L. Liu, F. Zhu, M. Yu, H. Wang, and L. Shao, “Star: A structure and texture aware retinex model,” *IEEE TIP*, vol. 29, pp. 5022–5037, 2020.
- [28] R. Liu, S. Cheng, L. Ma, X. Fan, and Z. Luo, “Deep proximal unrolling: Algorithmic framework, convergence analysis and applications,” *IEEE TIP*, vol. 28, no. 10, pp. 5013–5026, 2019.
- [29] H. Zhang and V. M. Patel, “Density-aware single image de-raining using a multi-stream dense network,” in *CVPR*, 2018, pp. 695–704.
- [30] T.-W. Hui, X. Tang, and C. Change Loy, “Liteflownet: A lightweight convolutional neural network for optical flow estimation,” in *CVPR*, 2018, pp. 8981–8989.
- [31] Y. Zhang, K. Li, K. Li, L. Wang, B. Zhong, and Y. Fu, “Image super-resolution using very deep residual channel attention networks,” in *ECCV*, 2018, pp. 286–301.
- [32] D. Berman, T. Treibitz, and S. Avidan, “Single image dehazing using haze-lines,” *IEEE TPAMI*, 2018.
- [33] R. Liu, L. Ma, Y. Wang, and L. Zhang, “Learning converged propagations with deep prior ensemble for image enhancement,” *IEEE TIP*, vol. 28, no. 3, pp. 1528–1543, 2019.
- [34] C. Li, J. Guo, F. Porikli, and Y. Pang, “Lightennet: a convolutional neural network for weakly illuminated image enhancement,” *PRL*, vol. 104, pp. 15–22, 2018.
- [35] R. Wang, Q. Zhang, C.-W. Fu, X. Shen, W.-S. Zheng, and J. Jia, “Underexposed photo enhancement using deep illumination estimation,” in *CVPR*, 2019, pp. 6849–6857.
- [36] V. Bychkovsky, S. Paris, E. Chan, and F. Durand, “Learning photographic global tonal adjustment with a database of input/output image pairs,” in *CVPR*, 2011, pp. 97–104.
- [37] M. Gharbi, J. Chen, J. T. Barron, S. W. Hasinoff, and F. Durand, “Deep bilateral learning for real-time image enhancement,” *ACM TOG*, vol. 36, no. 4, 2017.
- [38] W. Yang, S. Wang, Y. Fang, Y. Wang, and J. Liu, “From fidelity to perceptual quality: A semi-supervised approach for low-light image enhancement,” in *CVPR*, 2020, pp. 3063–3072.
- [39] Y. Zhang, X. Guo, J. Ma, W. Liu, and J. Zhang, “Beyond brightening low-light images,” *IJCV*, vol. 129, no. 4, pp. 1013–1037, 2021.
- [40] K. G. Lore, A. Akintayo, and S. Sarkar, “Llnet: A deep autoencoder approach to natural low-light image enhancement,” *Pattern Recognition*, vol. 61, pp. 650–662, 2017.
- [41] C. Chen, Q. Chen, J. Xu, and V. Koltun, “Learning to see in the dark,” in *CVPR*, 2018, pp. 3291–3300.

- [42] J. Cai, S. Gu, and L. Zhang, "Learning a deep single image contrast enhancer from multi-exposure images," *IEEE TIP*, vol. PP, no. 99, pp. 1–1, 2018.
- [43] S. Lim and W. Kim, "Dslr: Deep stacked laplacian restorer for low-light image enhancement," *IEEE TMM*, 2020.
- [44] K. Lu and L. Zhang, "Tbefn: A two-branch exposure-fusion network for low-light image enhancement," *IEEE TMM*, 2020.
- [45] K. Xu, X. Yang, B. Yin, and R. W. Lau, "Learning to restore low-light images via decomposition-and-enhancement," in *CVPR*, 2020, pp. 2281–2290.
- [46] C. Li, C. Guo, and C. L. Chen, "Learning to enhance low-light image via zero-reference deep curve estimation," *IEEE TPAMI*, 2021.
- [47] L. Xu, C. Lu, Y. Xu, and J. Jia, "Image smoothing via l0 gradient minimization," *ACM TOG*, 2011.
- [48] Z. Farbman, R. Fattal, D. Lischinski, and R. Szeliski, "Edge-preserving decompositions for multi-scale tone and detail manipulation," in *ACM TOG*, vol. 27, no. 3, 2008, p. 67.
- [49] C.-W. F. X. S. W.-S. Z. J. J. Ruixing Wang, Qing Zhang, "Underexposed photo enhancement using deep illumination estimation," in *CVPR*, 2019.
- [50] D. Min, S. Choi, J. Lu, B. Ham, K. Sohn, and M. N. Do, "Fast global image smoothing based on weighted least squares," *IEEE TIP*, vol. 23, no. 12, pp. 5638–5653, 2014.
- [51] S. Guo, Z. Yan, K. Zhang, W. Zuo, and L. Zhang, "Toward convolutional blind denoising of real photographs," in *CVPR*, 2019.
- [52] Z.-u. Rahman, D. J. Jobson, and G. A. Woodell, "Retinex processing for automatic image enhancement," *JEI*, vol. 13, no. 1, pp. 100–111, 2004.
- [53] S. Wang, J. Zheng, H.-M. Hu, and B. Li, "Naturalness preserved enhancement algorithm for non-uniform illumination images," *IEEE TIP*, vol. 22, no. 9, pp. 3538–3548, 2013.
- [54] K. Ma, K. Zeng, and Z. Wang, "Perceptual quality assessment for multi-exposure image fusion," *IEEE TIP*, vol. 24, no. 11, pp. 3345–3356, 2015.
- [55] V. Voniakakis, R. Kouskouridas, and A. Gasteratos, "On the evaluation of illumination compensation algorithms," *MTA*, vol. 77, no. 8, pp. 9211–9231, 2018.
- [56] A. Mittal, R. Soundararajan, and A. C. Bovik, "Making a completely blind image quality analyzer," *IEEE SPL*, vol. 20, no. 3, pp. 209–212, 2013.
- [57] B. Li, W. Ren, D. Fu, D. Tao, D. Feng, W. Zeng, and Z. Wang, "Benchmarking single-image dehazing and beyond," *IEEE TIP*, vol. 28, no. 1, pp. 492–505, 2018.
- [58] K. He, J. Sun, and X. Tang, "Single image haze removal using dark channel prior," *IEEE TPAMI*, vol. 33, no. 12, pp. 2341–2353, 2011.
- [59] B. Cai, X. Xu, K. Jia, C. Qing, and D. Tao, "Dehazenet: An end-to-end system for single image haze removal," *IEEE TIP*, vol. 25, no. 11, pp. 5187–5198, 2016.
- [60] Y. Qu, Y. Chen, J. Huang, and Y. Xie, "Enhanced pix2pix dehazing network," in *CVPR*, 2019, pp. 8160–8168.
- [61] W. Ren, L. Ma, J. Zhang, J. Pan, X. Cao, W. Liu, and M.-H. Yang, "Gated fusion network for single image dehazing," in *CVPR*, 2018, pp. 3253–3261.
- [62] X. Qin, Z. Wang, Y. Bai, X. Xie, and H. Jia, "Ffa-net: Feature fusion attention network for single image dehazing," in *AAAI*, vol. 34, no. 07, 2020, pp. 11908–11915.
- [63] J. Pan, J. Dong, Y. Liu, J. Zhang, J. Ren, J. Tang, Y.-W. Tai, and M.-H. Yang, "Physics-based generative adversarial models for image restoration and beyond," *IEEE TPAMI*, vol. 43, no. 7, pp. 2449–2462, 2020.
- [64] S. Zhao, L. Zhang, Y. Shen, and Y. Zhou, "Refinednet: A weakly supervised refinement framework for single image dehazing," *IEEE TIP*, vol. 30, pp. 3391–3404, 2021.
- [65] W. Ren, J. Pan, H. Zhang, X. Cao, and M.-H. Yang, "Single image dehazing via multi-scale convolutional neural networks with holistic edges," *IJCV*, vol. 128, no. 1, pp. 240–259, 2020.
- [66] A. Galdran, A. Alvarez-Gila, A. Bria, J. Vazquez-Corral, and M. Bertalmio, "On the duality between retinex and image dehazing," in *CVPR*, 2018, pp. 8212–8221.



**Long Ma** received the B.E. degree in information and computing science from Northeast Agricultural University, Harbin, China, in 2016. received the M.S. degree in software engineering at Dalian University of Technology, Dalian, China, in 2019. He is currently pursuing the Ph.D. degree in software engineering at Dalian University of Technology, Dalian, China. He is a reviewer for CVPR, ICCV, AAAI, ECCV, IEEE TIP, and IEEE TCSV. His research interests include computer vision and image enhancement.



**Risheng Liu** received his B.Sc. (2007) and Ph.D. (2012) from Dalian University of Technology, China. From 2010 to 2012, he was doing research as joint Ph.D. in robotics institute at Carnegie Mellon University. From 2016 to 2018, He was doing research as Hong Kong Scholar at the Hong Kong Polytechnic University. He is currently a full professor with the Digital Media Department at International School of Information Science & Engineering, Dalian University of Technology (DUT). He was awarded the "Outstanding Youth Science Foundation" of the National Natural Science Foundation of China. He serves as associate editor for Pattern Recognition, the Journal of Electronic Imaging (Senior Editor), The Visual Computer, and IET Image Processing. His research interests include optimization, computer vision and multimedia.



**Yiyang Wang** received the B.Sc. and Ph.D. degrees in mathematics from the Dalian University of Technology, in 2012 and 2017, respectively. She was holding a post-doctoral position at the Institute of Atmospheric Sciences, Fudan University and Shanghai Institute of Meteorological Science from 2017 to 2020. She is currently an associate professor with the College of Artificial Intelligence, Dalian Maritime University. Her main research interests include machine learning, optimization, and image processing.



**Xin Fan** received the B.E. and Ph.D. degrees in information and communication engineering from Xian Jiaotong University, Xian, China, in 1998 and 2004, respectively. He was with Oklahoma State University, Stillwater, from 2006 to 2007, as a post-doctoral research Fellow. He joined the School of Software, Dalian University of Technology, Dalian, China, in 2009. His current research interests include computational geometry and machine learning, and their applications to lowlevel image processing and DTI-MR image analysis.



**Zhongxuan Luo** received the B.S. degree in Computational Mathematics from Jilin University, China, in 1985, the M.S. degree in Computational Mathematics from Jilin University in 1988, and the Ph.D. degree in Computational Mathematics from Dalian University of Technology, China, in 1991. He has been a full professor of the School of Mathematical Sciences at Dalian University of Technology since 1997. His research interests include computational geometry and computer vision.